This article has been accepted for inclusion in a future issue of this journal. Content is final as presented, with the exception of pagination.

Design and Simulation of ISTTOK Real-Time Magnetic Multiple-Input Multiple-Output Control

Doménica Corona, Nuno Cruz, José Julio Emilio Herrera, Humberto Figueiredo, Bernardo B. Carvalho, Ivo S. Carvalho, Hugo Alves, and Horácio Fernandes

***Abstract*— Control of the plasma current and the position of its centroid and its shape is vital for obtaining advanced performance regimes in tokamak operation. For that aim, the use of poloidal magnetic coils for feedback control is essential. In this paper, a multiple-input multiple-output (MIMO) optimal control algorithm for the vertical and horizontal control position of the plasma current centroid at IST tokamak (ISTTOK) is presented. Using the ISTTOK magnetic system, the real-time control is made possible by the execution of generic application modules (GAMs), developed to be executed on the Multithreaded Application Real-Time executor ISTTOK controller. The design of the proposed MIMO controller is based on a state-space model of the ISTTOK magnetic response that has been identified from experimental data. Both the control design and the identification procedure rely on the reconstruction of the plasma centroid position computed by the magnetic probes (Mirnov coils) installed at ISTTOK. The centroid position is reconstructed in the Position GAM by numerical integration of the magnetic probes signals in the recently upgraded hardware based on the Advanced Telecommunications Computing Architecture. The effectiveness of the proposed control approach is presented comparing simulation results with experimental ones obtained using single-input single-output PID controllers. Moreover, due to the modularity of the ISTTOK control system, the proposed real-time reconstruction algorithm has been easily deployed on the plant, and the same approach will be adopted to test the MIMO controller in the future.**

***Index Terms*— Magnetic probes, Mirnov coils, multiple-input multiple-output (MIMO) controller, plasma centroid position, plasma current, poloidal magnetic coils, state-space model.**

I. Introduction

IST TOKAMAK (ISTTOK) a large aspect ratio tokamak operated at the Instituto de Plasmas e Fusão Nuclear Instituto Superior Técnico. One of its main features is the ac discharges capability which allows a much longer discharge [1]. A real-time control system was developed based on the Advanced Telecommunications Computing Architecture (ATCA) standard. The real-time control system is programmed on top of the Multithreaded Application Real-Time executor (MARTe) framework with a 100-μs control cycle which integrates the information gathered by all the tokamak real-time diagnostics to produce an accurate observation of the plasma parameters [2].

Magnetic diagnostics are integrated in ISTTOK to retrieve important plasma parameters such as the centroid position of the column and the plasma current. The reconstruction of these parameters is performed by hardware digital integration and programming blocks in the MARTe generic application modules (GAMs) [3], replacing a set of Mirnov coils that was previously used to retrieve the plasma centroid position with analogical integration [4].

The atomic elements of MARTe are the GAMs and all applications built using the framework are designed around these components. A GAM is a block of code implementing an interface specified in the C++ multiplatform real-time library named BaseLib2. Each GAM contains three communication points: one for configuration and two for data input and output [3].

Profiting from the modular nature of MARTe, the algorithms of each diagnostic data processing, discharge timing, context switch, control and actuators output reference generation, run on well-defined GAM blocks. This approach enables reusability of the code and simplifies simulation [5].

Control of the plasma current shape and its centroid position is a crucial control task in order to improve the performance of tokamak plasmas. This paper presents a twofold contribution: 1) a real-time reconstruction algorithm to estimate the plasma current centroid position using only the Mirnov coils installed at ISTTOK and 2) a proposal for a multiple-input multiple-output (MIMO) controller [6], [7] for the purpose of controlling the position of the plasma current centroid. The procedure used to identify a state-space model for the controller design starting from the ISTTOK experimental data is also provided [8], together with some simulation results.

A brief description of the overall ISTTOK control system is presented in Section II, while more details on the magnetic diagnostics are shown in Section III. The real-time algorithm implemented in the MARTe framework to reconstruct the plasma current intensity and current centroid position using the signals acquired from the Mirnov coils is described in Section IV. The proposed approach for model identification

Manuscript received October 27, 2017; revised January 31, 2018; accepted February 27, 2018. This work was supported by the Fundação para a Ciência e Tecnologia through the Instituto de Plasma e Fusão Nuclear, a research institute of Instituto Superior Técnico, and through the Ph.D. Grant, under Grant FCT-PD/BD/114306/2016. The review of this paper was arranged by Senior Editor S. J. Gitomer. *(Corresponding author: Doménica Corona.)*

D. Corona, N. Cruz, H. Figueiredo, B. B. Carvalho, I. S. Carvalho, H. Alves, and H. Fernandes are with the Instituto de Plasmas e Fusão Nuclear Instituto Superior Técnico, 1049-001 Lisbon, Portugal (e-mail: lilia.rivera@tecnico.ulisboa.pt; nunocruz@lei.fis.uc.pt; fernando@ipfn.tecnico.ulisboa.pt; bernardo.carvalho@tecnico.ulisboa.pt; ivo.carvalho@ipfn.ist.utl.pt; halves@ipfn.ist.utl.pt; hf@ipfn.tecnico.ulisboa.pt).

J. J. E. Herrera is with the Instituto de Ciencias Nucleares, Univesidad Nacional Autónoma de México, Mexico City 04510, Mexico (e-mail: herrera@nucleares.unam.mx).

Color versions of one or more of the figures in this paper are available online at http://ieeexplore.ieee.org.

Digital Object Identifier 10.1109/TPS.2018.2815282

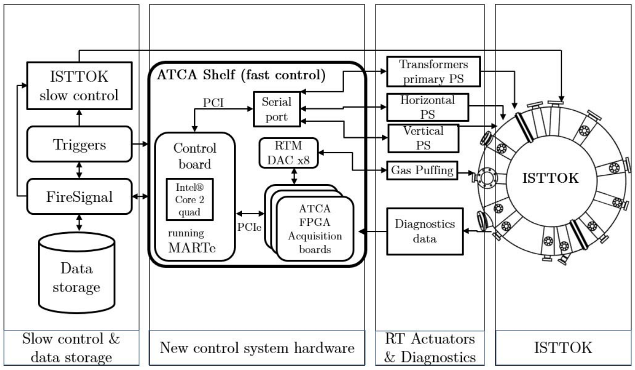

Fig. 1. ISTTOK overall control schematic. Data are acquired by the ATCA data acquisition boards, and decimated and transferred to the hosts every 100 μs.

and control is presented in Section V together with some preliminary simulation results. The control system was designed and simulated and is now under implementation to be tested in ISTTOK.

II. ISTTOK Control System

In this section, a brief description of the ISTTOK control system and the properties of the poloidal field (PF) coils are given.

The ISTTOK fast control system based on the ATCA standard was implemented maintaining the old ISTTOK slow control system, based on control boards using the peripheral component interconnect bus standard, while completely reformulating the fast controller. The ATCA hardware is currently used to control the plasma current in real time with data provided by Rogowsky coils. The plasma centroid position is roughly estimated with electrostatic probes, and therefore, its real-time control is fairly ineffective [9]. Fig. 1 depicts the schematic of the implemented control system showing the integration of all diagnostics and power supplies for control position in the fast control system.

One of the ISTTOK control system main features is the automatic inversion of the plasma current direction when the iron core saturates while maintaining a residual gas ionization during the reversal process, which allows a much longer discharge with no use of auxiliary heating [10], [11].

A. Poloidal Field Coils

The control of the plasma current and centroid position is made possible by using a feedback closed loop which operates the power supplies of the PF coils depicted in Fig. 2. The ohmic heating (OH) coils of the tokamak transformer, also referred in this paper as primary windings of the tokamak transformer or simply primary coils, are represented in white, vertical field coils in yellow, and horizontal field coils in green. The PF and the OH coils power supplies have their own independent current feedback control and communicate by means of an optical link with the main control system. The current-control algorithm is based on a bang-bang controller with feedback in current [12].

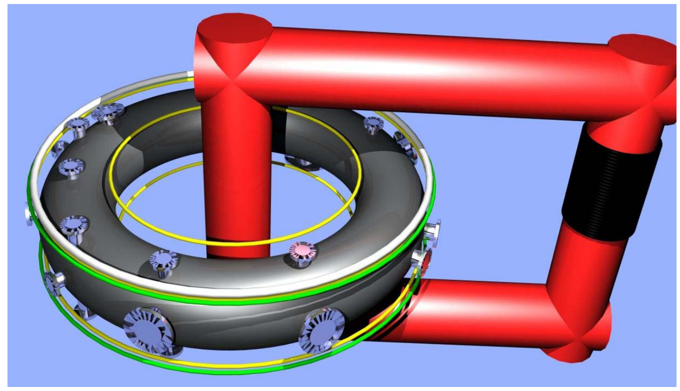

Fig. 2. ISTTOK PF coils [13].

Fig. 3(a)–(c) shows the magnetic surfaces and field lines generated by the currents passing through the primary, horizontal, and vertical PF coils. Fig. 3 also shows the poloidal cross section of the vacuum chamber and the position of the PF coils.

Since the ISTTOK central solenoid is not being used as the primary winding to create the toroidal electric field responsible for creating and maintaining the plasma current I_p, as shown in Fig. 3(a), two outer coils are used for this purpose and an additional vertical field is produced [14]. The pure vertical PF coils, depicted in Fig. 3(c), produce a field that either add or compensate the field generated by the primary coils in order to obtain the desired vertical field.

III. Magnetic Diagnostics

A description of the calibration process and offset subtraction on the magnetic probes numerical integrated signals and also the experimental modeling for the measurements of the external magnetic fluxes are detailed in this section.

ISTTOK magnetic diagnostics include 12 probes (Mirnov coils) set along the poloidal cross section and positioned inside the vacuum chamber, as shown in Fig. 4. Each coil has an area of 25 mm^2 and 50 turns. The plasma current and horizontal and vertical positions are reconstructed through the integrated magnetic flux measured by the Mirnov coils.

The set of 12 magnetic probes is connected to a carrier board where each channel is connected to a plugged-in analogic to digital convertor (ADC) module. These modules are connected digitally to a XILINX Virtex-4 FPGA (field-programmable gate array) which performs the necessary digital signal processing.

Analog integration of magnetic signals is affected by voltage offsets and drifts on the components and wiring. Even very low offsets integrated during a long period of time may appear as a noticeable deviation of the integrated signals. In this paper, we implemented a solution for the integration of the Mirnov coil signals that makes use of a phase inverter (chopper) to periodically reverse the input signals before active amplification, filtering, and sampling in the ADC, as shown in Fig. 5. The modulation of the signals prior to any electronic amplification and the reconstruction of the digital equivalent of the signal after the digitalization allows for the average of the electronics offset (EO) to be expected to converge to zero

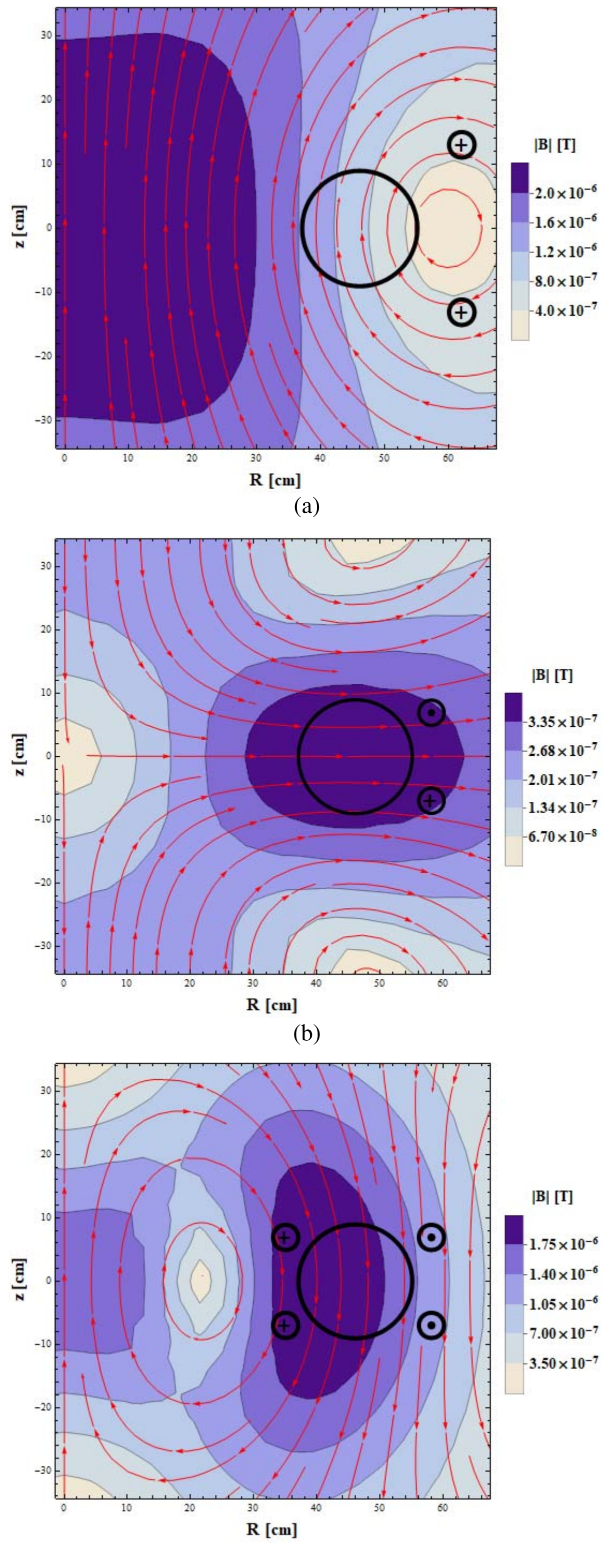

Fig. 3. Magnetic field lines, magnetic surfaces created by the currents in the primary, horizontal, and vertical PF coils, and directions of the currents in the coils. (a) Primary PF coil (OH coil). (b) Horizontal PF coil. (c) Vertical PF coil.

in the integration process, as long as its value is steady enough over at least two inversion periods.

Correction of the EO is achieved by performing an average on raw data values. Fig. 6 shows the EO offsets in one of

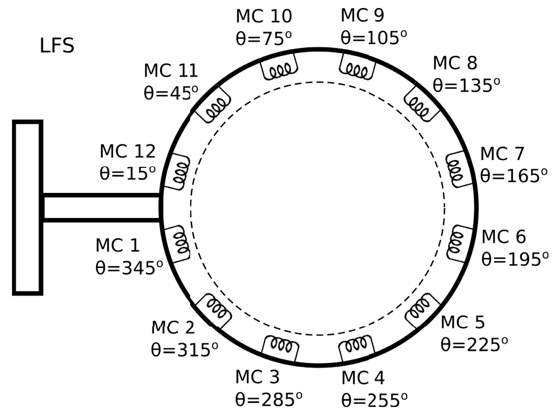

Fig. 4. ISTTOK Mirnov coil locations. Set of 12 tangent magnetic probes distributed along the poloidal direction. Left: low field side.

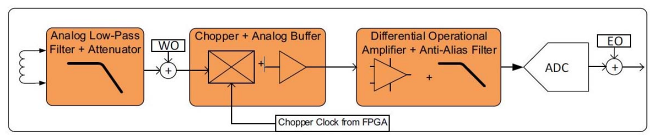

Fig. 5. ADC module diagram depicting the influence of the WO and EO offsets [15].

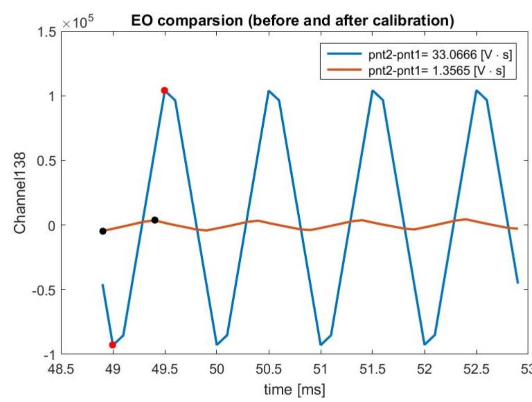

Fig. 6. EO comparison in Mirnov coil # 10 (Channel 138) before (blue line)/after (orange line) calibration.

the magnetic probes before and after the calibration process showing a substantially smaller value of the EO on the calibrated signal. These values are the characteristic of the modules and the acquisition board [16].

In addition, a second offset also appears before the chopper. It is shown in Fig. 5 as wiring offset (WO), and it may be originated either inside the module or in the external wiring, connectors and soldered parts, mainly due to uncompensated thermocouple effects, external interference or radiation effects [15]. Unfortunately, the WO offset will not be averaged by the chopping method, despite this, and assuming WO is stable enough, it can be precisely measured before any magnetic field is applied and later compensated during the code execution. By starting the acquisition process of the magnetic probes signals 4 ms before the magnetic fields are applied, the WO is computed as an approximation of a linear curve and then subtracted from the measured signals. Through the characterization of the acquisition process on the

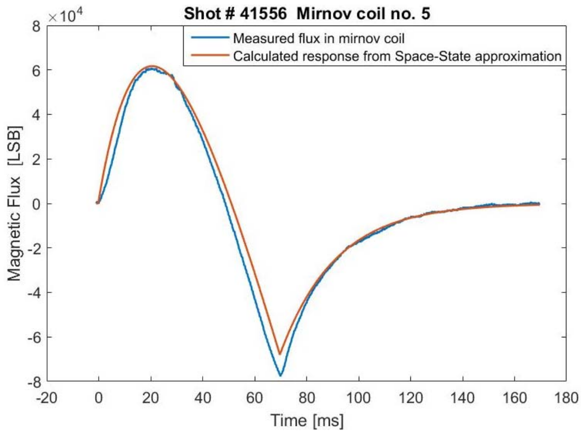

Fig. 7. External magnetic flux measured on a Mirnov coil and the comparison of the estimated flux through a retrieved state-space model.

probes for different time windows (1 s $\gtrsim t \gtrsim$ 50 ms), it was determined that this period of 4 ms before the magnetic fields are applied is long enough to determine the WO offsets.

A. External Poloidal Flux Measurement

Since the measurements from the set of Mirnov coils are the sum of the poloidal magnetic fields generated by the plasma and the currents in the PF coils (primary, vertical, and horizontal systems), in order to have an accurate plasma position reconstruction, it is necessary to subtract, during the Position GAM execution, an approximation of the magnetic flux generated by the coils.

A first-order state-space model for each coil is proposed and characterized through the System Identification MATLAB Toolbox [17]. The obtained state-space discrete equations are programmed in the Position GAM and computed on every MARTe control cycle, and thus, the contribution of magnetic flux due to the PF coils is subtracted in real time [18, Ch. 6].

Performing plasmaless discharges at ISTTOK, the Mirnov coils were individually characterized with the influence of the external magnetic fluxes. Fig. 7 shows the measured magnetic flux in the Mirnov coil no. 5 and its reconstruction through the experimental approximation process.

IV. Plasma Current and Centroid Position Reconstruction

This section outlines the algorithms for computing the reconstruction of the plasma current and the vertical and radial position of its centroid. Some comparisons between diagnostics and the approach on the reconstruction of the signals are presented.

The magnetic field in each one of the Mirnov coils can be obtained from the expression

$$H(t) = -\frac{1}{\mu_0 N A}\int_o^t v_{\text{mirnov}}(\tau)d\tau \tag{1}$$

where N is the number of turns of the probe and A is its area. Since the integration of the voltage measured in the probes is performed by the board, after the WO offset correction,

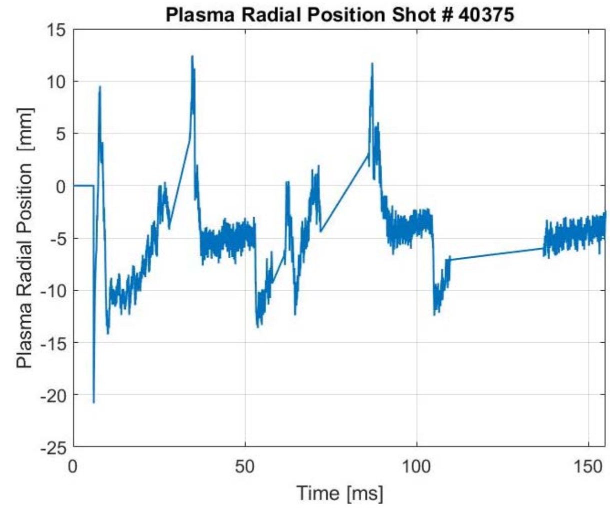

(a)

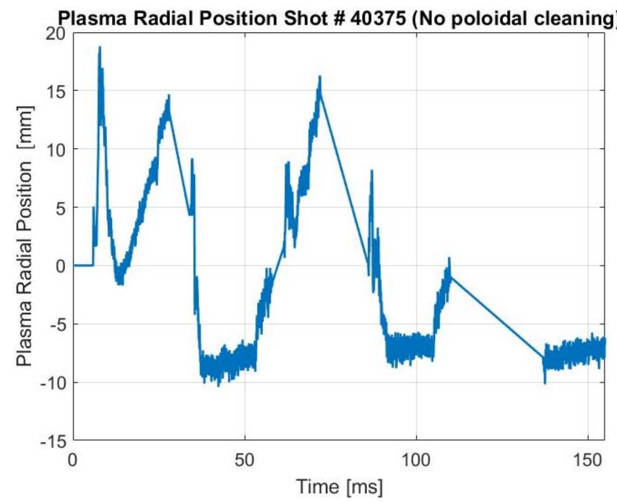

(b)

Fig. 8. Plasma current centroid radial position comparison. (a) Radial current centroid position reconstruction with subtraction of the external magnetic fluxes. (b) Radial current centroid position reconstruction without subtraction of the external magnetic fluxes.

the value of the plasma magnetic flux can be introduced directly substituting in the integral of (1).

Following the centroid algorithm for a circular plasma and considering ISTTOK is a large aspect ratio tokamak, the vertical and horizontal plasma centroid position can be obtained through:

$$R = \frac{\sum_{i=1}^{i=12} R_{\text{probe}} \times H_i(t)}{\sum_{i=1}^{i=12} H_i(t)} \tag{2}$$

$$z = \frac{\sum_{i=1}^{i=12} z_{\text{probe}} \times H_i(t)}{\sum_{i=1}^{i=12} H_i(t)} \tag{3}$$

where R_{probe} and z_{probe} are the radial and vertical coordinates of the probes, respectively, as depicted in Fig. 4. A similar algorithm that describes how to retrieve the vertical position of the plasma centroid in diverted plasmas can be found in [19].

Figs. 8 and 9 show the obtained radial and vertical current centroid position and a comparison of the results with and

This article has been accepted for inclusion in a future issue of this journal. Content is final as presented, with the exception of pagination.

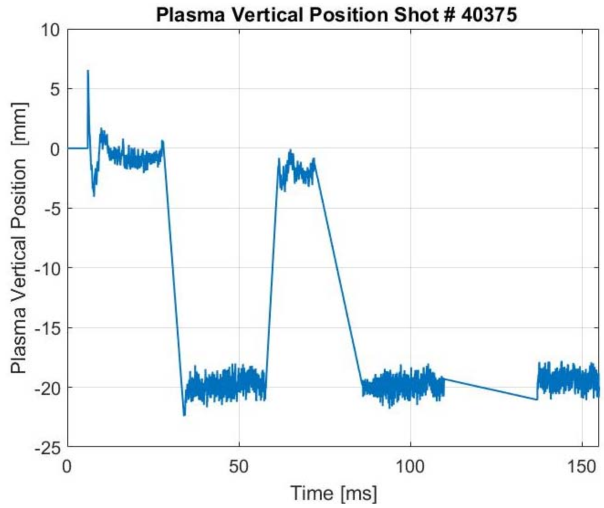

(a)

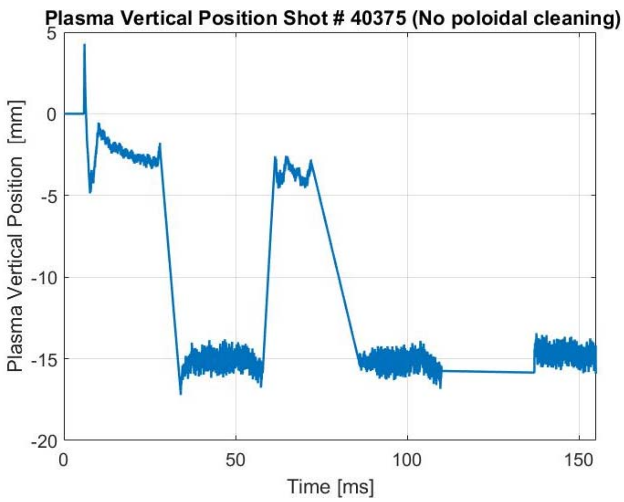

(b)

Fig. 9. Plasma current centroid vertical position comparison. (a) Vertical current centroid position reconstruction performing a cleaning process of the external magnetic fluxes. (b) Vertical current centroid position reconstruction without a cleaning process of the external magnetic fluxes.

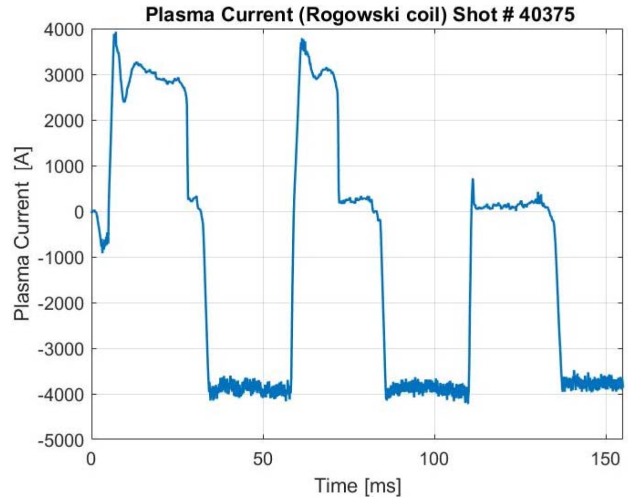

(a)

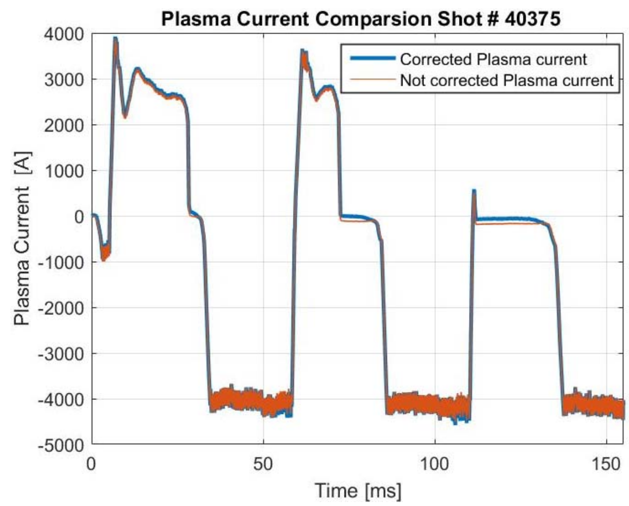

(b)

Fig. 10. Plasma current. (a) Plasma current measured in the Rogowski coil. (b) Comparison of the plasma current reconstruction through the magnetic probes with and without the subtraction of the external magnetic fluxes.

without the subtraction of the external magnetic fluxes measured in the magnetic probes.

The expression for the reconstruction of the plasma current is given by

$$I_p = \frac{2\pi r_{\text{Mirnov}}}{N} \sum_{i=1}^{i=12} H_i(t) \tag{4}$$

where r_{mirnov} is the radial distance from each one of the Mirnov coils to the center of the chamber (9.35 cm). Fig. 10(a) shows the plasma current measured with the Rogowski coil and Fig. 10(b) shows a comparison of the plasma current reconstructed through the measurements in the magnetic probes with and without the subtraction of the magnetic external fluxes.

V. State-Space and Control Modeling

A brief description of the experimental model identification and concepts on multivariable linear systems and feedback control are given in this section in order to propose an MIMO controller for the position of the plasma current centroid. Results from the simulated MIMO controller compared with the ones from existing single input single output (SISO) are also presented.

The experimental reconstruction of a state-space model of the tokamak makes possible to retrieve a model approximation that allows the usage of other control techniques besides the already implemented SISO-PID controllers. This property is of the utmost importance in the case of the ISTTOK tokamak, because the data on the mechanical characteristics of the vacuum chamber are not available and the exact geometrical configuration of the PF coils is very hard to retrieve due to machine construction constraints related to its small size.

The interaction between the plasma and the PF coils can be described by a set of nonlinear partial differential equations, whereas the controller design techniques are based upon the availability of ordinary differential equation models, usually linear, time invariant, and low order. The main problem is

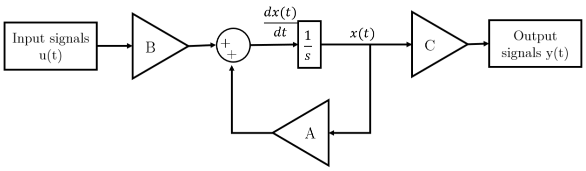

Fig. 11. State-space model block diagram.

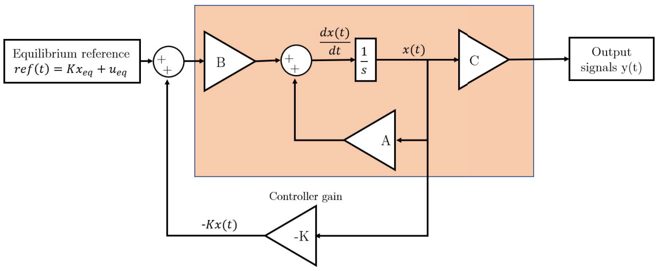

Fig. 12. State-space model block diagram with a gain matrix K in closed loop.

the introduction of physical simplifying assumptions and the use of approximate numerical methods so as to obtain a sufficiently detailed model that is capable of grabbing the main physical phenomena and is simultaneously reasonably simple to make the controller design possible [20]. A model in state-space variables relates the variations of the PF currents to the variations of the outputs around a given equilibrium.

State-space models use state variables to describe a system by a set of first-order differential or difference equations rather than by one or more nth-order differential or difference equations. Equations (5) and (6) describe a state-space model and they are called the internal description of linear systems, where A is named the state or system matrix, B is the input matrix, C is the output matrix, and D is the feedforward matrix [18]. Fig. 11 shows a block diagram of a generic state-space model, considering the system model does not have a direct feedthrough (D is a zero matrix)

$$\dot{x}(t) = Ax(t) + Bu(t) \tag{5}$$

$$y(t) = Cx(t) + Du(t). \tag{6}$$

From the control theory, it is possible to reconstruct a state-space model based on the behavior of the inputs and outputs in an open-loop system [8], [21]. In order to make a first approximation of an MIMO controller, a state-space model of the system was obtained using an estimation subspace method through the System Identification MATLAB Toolbox. The experimental data of the currents in the PF coils (input signals) and the radial and vertical plasma current centroid positions (output signals) obtained from open-loop discharges were used to retrieve a system with an optimal number of states [17].

A. Control Technique

The linear quadratic regulator (LQR) is a well-known design technique that provides practical feedback gains. For the derivation of the LQR, we assume that the system plant is

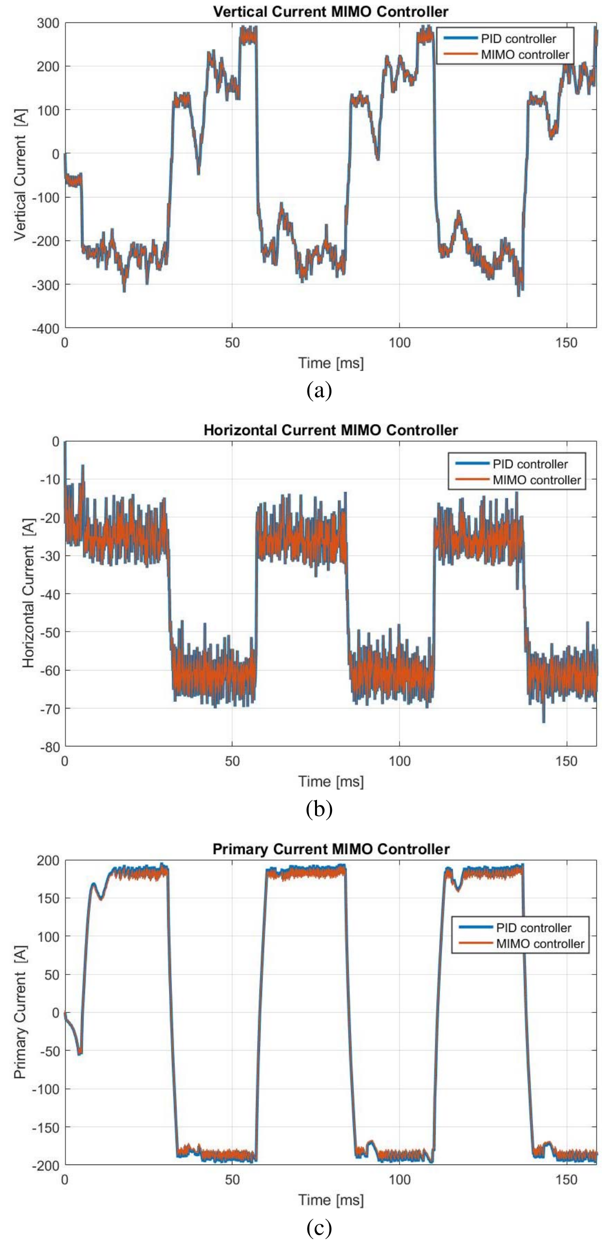

Fig. 13. Comparison of the PF coils currents controllers. (a) Current in the vertical PF coil from PID and MIMO optimal controller. (b) Current in the horizontal PF coil from PID and MIMO optimal controller. (c) Current in the primary PF coil from PID and MIMO optimal controller.

written in a state-space form and the dynamics of the closed-loop system are then written as

$$\dot{x}(t) = (A - BK)x(t) + BKx_{\text{eq}}. \tag{7}$$

For the control design, two positive definite matrices named Q and R are proposed, and Q will be related with the penalties in time and transient response and R with the inputs. Afterward, the values of the matrices are replaced in the Riccati equation for an LQR design [22]. This equation is the matrix algebraic Riccati equation (8), whose solution P is needed to compute the optimal feedback gain K. The Riccati equation is easily solved by standard numerical

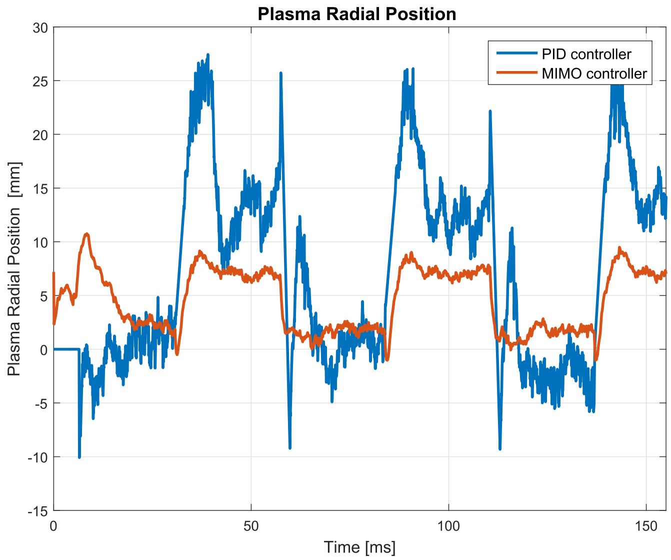

Fig. 14. Plasma centroid radial position. Positions retrieved from a discharge with PID controllers (blue line) and an MIMO optimal controller (orange line).

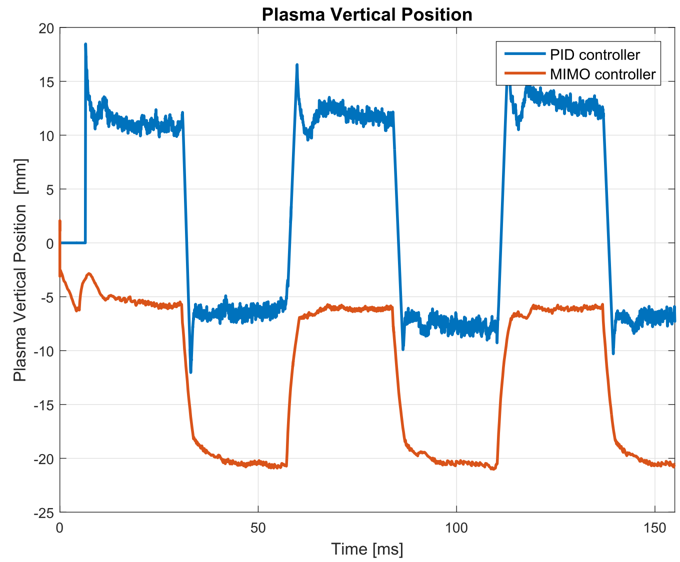

Fig. 15. Plasma centroid vertical position. Positions retrieved from a discharge with PID controllers (blue line) and an MIMO optimal controller (orange line).

tools in linear algebra

$$\mathrm{PA} + A^{\mathrm{T}}P + Q - \mathrm{PBR}^{-1}B^{\mathrm{TP}} = 0. \tag{8}$$

The LQR generates a static gain matrix K, which is not a dynamical system. Hence, the order of the closed-loop system is the same as that of the plant. Fig. 12 shows the block diagram of the state-space model with a closed loop multiplied by the calculated gain matrix K and a reference vector related to the equilibrium of the system.

The implementation of the control algorithm on real time will be performed in the Controller GAM, multiplying the calculated gain matrix K by the estimated states of the system and executing the feedback control loop on each MARTe cycle.

B. Control Results

The reference vectors given as inputs of the system through (9) were designed based on the vertical, horizontal, and primary PF coils currents from a standard shot controlled by a set of three PID controllers. These signals were set as the input reference (u_{eq}) to the feedback loop at the state-space system

$$\mathrm{ref}(t) = Kx_{\mathrm{eq}} + u_{\mathrm{eq}}. \tag{9}$$

Fig. 13 shows the comparison of the current values in the PF coils between a discharge where the control loop was done by a set of SISO PID controllers and the ones from the optimal MIMO controller modeled, proving that the output signals from the MIMO controller were able to track the given references.

Figs. 14 and 15 show the plasma current centroid positions comparing the measurements from a PID controlled discharge in the blue line with an MIMO optimal controller in the orange line. The main fact to point out is the tracking in both signals of the alternation in the position due to the ac discharge and the more stable response for each semicycle with the MIMO optimal controller. The radial position graph also depicts a lesser variation in the centroid position between the positive and negative cycles. The difference in the offset at the vertical PID and MIMO output positions takes place due to the initial conditions retrieved from the experimental data.

VI. Conclusion

ISTTOK holds a flexibility that allows to disable the feedback controllers in the PF coils power supplies setting a desired waveform in order to perform open-loop shots. These shots were successfully used to retrieve important information of the system plant, such as an experimental model which can be compared with a future theoretical model and, in turn, contribute to compare control results originated from experimental and theoretical models.

Plasma position results based on an MIMO controller modeled from a retrieved state-space model are consistent with the measured results in a PID controlled discharge. Furthermore, the plasma position retrieved from the MIMO controller shows an increased stability response during each plasma current semicycle in comparison with the PID controllers, suggesting that the replacement of the SISO controllers in the system is a suitable option.

Future work in ISTTOK includes an attempt for a first theoretical state-space modeling approximation of the system for the design of a controller and the comparison with the presented control designed on the basis of an experimental retrieved model.

References

[1] H. Fernandesa, C. A. F. Varandas, J. A. C. Cabral, H. Figueiredo, and R. Galvãob, "Engineering aspects of the ISTTOK operation in a multicycle alternating flat-top plasma current regime," *Fusion Eng. Des.*, vol. 43, no. 1, pp. 101–113, Oct. 1998.

[2] I. S. Carvalho *et al.*, "ISTTOK control system upgrade," *Fusion Eng. Des.*, vol. 88, nos. 6–8, pp. 1122–1126, 2013.

[3] A. C. Neto *et al.*, "MARTe: A multiplatform real-time framework," *IEEE Trans. Nucl. Sci*, vol. 57, no. 2, pp. 479–486, Apr. 2010.
[4] D. F. Valcárcel *et al.*, "Validation of ISTTOK plasma position controller," in *Proc. AIP Conf.*, vol. 996. 2008, pp. 291–296.
[5] I. S. Carvalho *et al.*, "ISTTOK real-time architecture," *Fusion Eng. Des.*, vol. 89, no. 3, pp. 195–203, 2014.
[6] B. D. O. Anderson and J. B. Moore, *Optimal Control: Linear Quadratic Methods*. North Chelmsford, MA, USA: Courier Corporation, 2007.
[7] S. Skogestad and I. Postlethwaite, *Multivariable Feedback Control: Analysis and Design*. New York, NY, USA: Wiley, 2007.
[8] L. Ljung, *System Identification: Theory for the User* (Prentice-Hall Information and System Sciences Series). Englewood Cliffs, NJ, USA: Prentice-Hall, 1999.
[9] I. S. Carvalho, H. Fernandes, P. Duarte, C. Silva, H. F. C. Figueiredo, and T. Hekkert, "ISTTOK real-time control assisted by electric probes," *J. Phys, Conf. Ser.*, vol. 591, no. 1, p. 012008, 2015.
[10] G. O. Ludwig, P. Rodrigues, and J. P. S. Bizarro, "Tokamak equilibria with strong toroidal current density reversal," *Nucl. Fusion*, vol. 53, no. 5, p. 053001, 2013.
[11] Y. Hu, "Tokamak plasma equilibria with a zero total toroidal current," *Phys. Plasmas*, vol. 15, no. 2, p. 022505, 2008.
[12] I. S. Carvalho *et al.*, "Real-time control for long ohmic alternate current discharges," *Fusion Eng. Des.*, vol. 89, no. 5, pp. 576–581, 2014. [Online]. Available: http://dx.doi.org/10.1016/j.fusengdes.2014.03.029
[13] I. S Carvalho *et al.*, "Real-time control for long ohmic alternate current discharges," Ph.D. dissertation, Inst. Superior Técnico, Inst. Plasmas Fusão Nucl., Univ. Lisbon, Lisbon, Portugal, 2013.
[14] O. Mitarai *et al.*, "Plasma current start-up experiments without a central solenoid in the iron core STOR-M tokamak," *Nucl. Fusion*, vol. 55, no. 6, p. 063034, 2015.
[15] B. Carvalho *et al.*, "Design, implementation and commissioning of ATCA based high-speed multichannel data acquisition systems for magnetic diagnostics in W7-X," in *Proc. 11th IAEA Tech. Meeting Control, Data Acquisition, Remote Participation Fusion Res.*, Greifswald, Germany, May 2017, pp. 1–5.
[16] B. Carvalho, M. Zilker, and T. Hekkert, "Test campaign of phase-modulated input digital integrator using the 2MSPS ATCA data acquisition system," Inst. Plasmas Fusão Nucl., Greifswald, Germany, Internal Tech. Rep., 2013.
[17] L. Ljung, *System Identification Toolbox: User's Guide*. Natick, MA, USA: MathWorks, 2017. [Online]. Available: www.mathworks.com/help/pdf_doc/ident/ident.pdf
[18] C.-T. Chen, *Linear System Theory and Design*. London, U.K.: Oxford Univ. Press, 1999.
[19] T. Bellizio *et al.*, "Control of elongated plasma in presence of ELMs in the JET tokamak," *IEEE Trans. Nucl. Sci.*, vol. 58, no. 4, pp. 1497–1501, Aug. 2011.
[20] M. Ariola and A. Pironti, *Magnetic Control of Tokamak Plasmas*, 2nd ed. Cham, Switzerland: Springer, 2016.
[21] M. Verhaegen, "Identification of the deterministic part of MIMO state space models given in innovations form from input-output data," *Automatica*, vol. 30, no. 1, pp. 61–74, 1994.
[22] P. Dorato, V. Cerone, and C. T. Abdallah, *Linear-Quadratic Control: Introduction*. London, U.K.: Simon Cowell, 1994.

Doménica Corona is currently pursuing the Ph.D. degree from the Advanced Program in Plasma Science and Engineering, Universidade de Lisboa, Lisbon, Portugal.

Her current research interests include magnetic control for ISTTOK tokamak and control applications for JT-60SA.

Nuno Cruz has focused on diagnostics and control algorithm development and control and data acquisition systems integration for several fusion devices, including JET, ITER, Tokamak à configuration variable (TCV), and JT-60SA. His current research interests include the design and development of high performance software and algorithms for the ITER Radial Neutron Camera, algorithms for edge-localized mode mitigation using vertical plasma kicks in TCV, optimal control for plasma vertical stabilization for TCV, and magnetic control tools for JT-60SA.

José Julio Emilio Herrera received the Physicist title, and the master's and Ph.D. degrees in physics from the Facultad de Ciencias, Universidad Nacional Autónoma de México (UNAM), México, in 1975, 1976, and 1979, respectively. His Ph.D. dissertation was on the systematics of the nuclear masses and the shell model.

He is currently a Titular Researcher at the Instituto de Ciencias Nucleares, UNAM, where he was a Lecturer with the Facultad de Ciencias. More recently, he has become involved in the exploration of symbiotic fission-fusion scenarios. His current research interests include dense magnetized plasmas, plasma physics and controlled fusion, related to equilibrium and stability in toroidal confinement plasmas.

Dr. Herrera has been a member of the International and Program Committees, such as the International Atomic Energy Agency (IAEA) Conference in Fusion Research in 2004, 2006, and 2012, the IAEA Technical Meeting on Research using Small Fusion Devices in 2005, 2007, and 2014, the International Congress in Plasma Physics from 1996 to 2004, and 2012, and the Latin American Workshop on Plasma Physics from 1988 to 2010, which he organized in Mexico in 1992, 2005, and 2017. He has been the Founding President of the Divisions of Fluid Dynamics and Plasma Physics with the Sociedad Mexicana de Física, and a Deputy Editor of its bulletin from 2010 to 2012. He currently serves on the editorial board of the *Revista Mexicana de Física*.

Humberto Figueiredo, photograph and biography not available at the time of publication.

Bernardo B. Carvalho received the Ph.D. degree in physics engineering from the Instituto Superior Tecnico, Lisbon, Portugal, in 2003.

He was a Chief Engineer with the European Shock-Tube for High Enthalpy Research Lab., Instituto Superior Técnico, Lisbon. He coordinates the control and data acquisition (CODAC) systems on the ISTTOK tokamak. His current research interests beyond CODAC for fusion devices include electronic instrumentation, field-programmable gate array data processing, magnetic probes, and MHD diagnostics.

Ivo S. Carvalho received the B.S., M.S. and Ph.D. degrees in physics engineering from the Instituto Superior Tecnico (IST), Lisbon, Portugal, in 2004, 2008, and 2013, respectively.

He has been a member of the JET Plasma Operations Group since 2014 as a secondee from IST. His scientific research started in 2004 in the real-time control and data acquisition area and expanded to the areas of machine operation and discharge performance optimization. Some scientific highlights include the extension of the ISTTOK tokamak alternate current discharges beyond one second of operation and the operation of the JET tokamak as a session leader.

Hugo Alves, photograph and biography not available at the time of publication.

Horácio Fernandes received the Ph.D. degree in physics engineering from the Instituto Superior Tecnico, Lisbon, Portugal, in 1997.

He coordinates the activity on the tokamak ISTTOK. He is currently the Chair of the Experimental Physics Group, Instituto de Plasmas e Fusão Nuclear, Instituto Superior Técnico, Lisbon. His scientific research is focused on fusion devices diagnostics and real-time control and operation. He has started to operate one of the earlier existing remote controlled physics laboratories in operation since 1999 related to his interest in electronic instrumentation. He also maintains regular participation in science outreach.

Dr. Fernandes is currently a member of the Technical Advisor Panel at F4E (the European Agency for ITER). He is a Research Coordinator of International Atomic Energy Agency.